Detection and analysis of degradation in the physical and electrical parameters in the PV cell

R. KHENFER[a,b], M. MOSTEFAI[a], S. BENAHDOUGA[b], A. EDDIAI[c,*]
[a]*LAS Laboratory, University Setif I, Sétif, Algeria*
[b]*Mohamed El Bachir El Ibrahimi University, BBA, Algeria.*
[c]*Laboratory of Physics of Condensed Matter (LPMC), Faculty of Sciences Ben M'sik, University Hassan II Mohammedia-Casablanca, Morocco.*

In this paper, we propose a method of analysis and detection degradation of physical and electrical parameters in photovoltaic cell. This method incorporates the stages of detection, localization and identification. For modeling PV panels, we used the two-diode model. Concerning the detection and localization, we used a limited number of voltage sensors. Also for the identification, we use the method of analysis of the I-V curve of the PV cell. By using this method, we can identify degradation due to climatic conditions as a partial shade, and the increase in the series resistance due to the corrosion or bad contact between cells, with examination of the presence of inflection points and calculate the second derivative of the error between the I-V characteristic with and without defects. The obtained simulation results showed the effectiveness of the proposed diagnosis method and the model used.

(Received May 14, 2014; accepted July 10, 2014)

Keywords: PV cell, Location and identification, Two-diode model, I-V characteristic analysis

1. Introduction

The great need of energy, require the recovery of energy available in our environment typical ambient energies include sunlight, mechanical energy, thermal energy, and RF energy [1, 2]. Converting ambient energy into electrical energy has attracted much interest in both the military and commercial sectors [3]. One of the most important sources of energy is the photovoltaic power (PV).

The photovoltaic power generation has widely spread in different applications ranging from space systems to the residential and commercial installations in buildings, telecommunication stations, power plants, and industrial applications [4].

During operation, a PV generator is subject to several defects. The most commonly encountered defect in the PV generator is the partial shade failure. This defect greatly minimizes the output power and makes the control of the converters ineffective; because the power delivered by the generator may have several maxima [5-6].This can happen, in particular, when the protective diodes (bypass diodes) of the PV cells are closed. Another defect that has the same effect as the defect of partial shade is the failure of increase in the series resistance Rs. The series resistance is a parameter to modeling of the photovoltaic cell. It represents the contact resistance between metal, semiconductor and the resistance of the semiconductor material.

Also, the operation of a PV generator in the presence of several defects and anomalies causes a decrease in the performance or total unavailability of the system. All these adverse consequences are obviously going to reduce productivity, and therefore reduce the performance of the plant, increase the cost of maintenance to make the system operating in normal state.

To minimize the unavailability period and maximize the performance and efficiency of PV systems, the diagnosis and the monitoring of PV system operation are essential.

Most of the works on fault diagnosis of PV presented in the literature use the model of a single diode of the PV cell [7-12]. Hence using other models for diagnosis such as a two-diode model is needed.

This work focuses on the diagnosis of the partial shade defect, a failure of increase the series resistance and their effects on the I-V characteristic in the DC side of a photovoltaic generator. This paper is organized into six sections:

Section 2 describes the modeling of a PV panel using a two-diode model which allows us to present the effect of partial shading and the defect of increasing of series resistance on I-V characteristic of the panel.

Section III provides a method of detecting and locating defects mentioned above. Section 4 deals with the method of fault identification by analysis of the curve I-V. Section 5 presents the different simulation results, and finally, section 6 concludes the paper.

2. PV model for two-diodes

Many electrical models are available in the literature to model the curves I-V of the PV modules, in particular the single-diode model. The single diodes models were based on the assumption that loss of recombination in the

depletion region is absent. In a solar cell, recombination represents a substantial loss that cannot be properly modeled using a single diode. The review of this loss results in a more accurate model known as a model for two-diodes [13-15], this model is shown in Fig. 1.

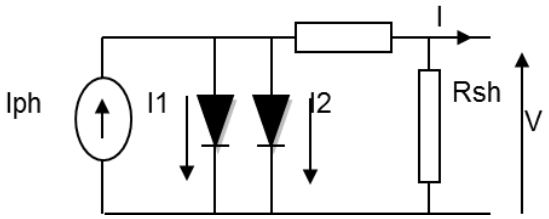

Fig.1. Equivalent circuit of PV cell with two- diodes.

A photovoltaic module PV consists of several cells in series. Thus, if all cells are identical, the global I-V curve can readily be determined by adding up the voltages of each cell.

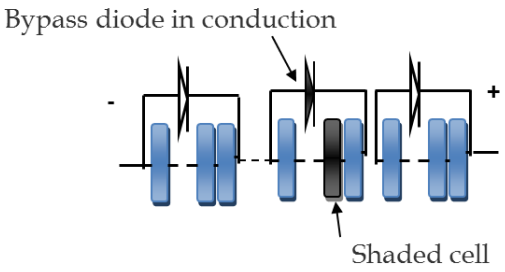

Fig.2. A branch cell with a PV cell shaded and a protection diode in conduction

Under real operating conditions, if the PV cells are slightly different from each other or if they are not uniformly illuminated (partial shade), the voltage at the terminals of the cells concerned is negative causing the conduction of the diode bypass fig. 2. The determination of the I-V curve in this case requires a specific model.

The model used is a double diode model that considers the inverse characteristic of the PV cell to present the operation under conditions of partial shade and increased series resistance [16,17].

The electrical current produced by the cell and presented by fig. 1, has the following expression:

$$I = I_{ph} - I_{01}\left(e^{\frac{q(v+IR_s)}{n_1 kT}} - 1\right) - I_{02}\left(e^{\frac{q(v+IR_s)}{n_2 kT}} - 1\right) - \left(\frac{v+IR_s}{R_{sh}}\right) \quad (1)$$

Where the first term I_{ph} is the photocurrent, the ideality factor n_1, n_2 (taken respectively equal to 1 and 2), I_{01}, I_{02} are the saturation currents for the diode respectively one and two are given with [17]:

$$I_{01} = C_{01}.T^3.e^{\frac{-E_{gap}}{n_1.k.T}} \quad (2)$$

$$I_{02} = C_{02}.T^{5/2}.e^{\frac{-E_{gap}}{n_2.k.T}} \quad (3)$$

R_s is the series resistance, R_{sh} is the shunt resistance, and k is the Boltzmann constant. q is the elementary charge, T is the temperature, The photo current is equal to:

$$I_{ph} = I_{ph,STC}.\left(\frac{G}{G_{STC}}\right).\left[1+\alpha_1\left(T-T_{STC}\right)\right] \quad (4)$$

G is a solar illumination on the module and STC is the standard test conditions, to consider the shading effect, the PV module is divided into two equal parts, each part has a group of cells connected in parallel with a bypass diode and each part behaves as a single module Fig. 3.

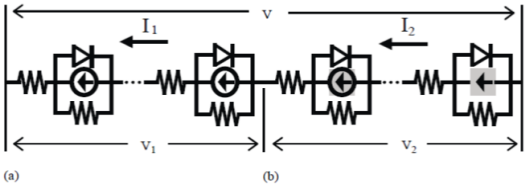

Fig.3. Equivalent circuit of a PV module with shaded PV cells, (a) normal PV cells (m1 cells), (b) shaded PV cells (m2 cells). [17]

The characteristic of a PV module with shaded cells is simulated by introducing an additional term that takes account the falling of the diode at high negative voltages. Thus:

$$I = I_1 = I_2 \quad (5)$$

$$v = v_1 + v_2 \quad (6)$$

then:

$$I_1 = I_{ph,1} - I_{01}\left(e^{\frac{q(v_1+I_1R_s)}{n_1 kT}} - 1\right) - I_{02}\left(e^{\frac{q(v_1+I_1R_s)}{n_2 kT}} - 1\right) - \left(\frac{v_1+I_1R_s}{R_{sh}}\right) \quad (7)$$

and

$$I_2 = I_{ph,2} - I_{01}\left(e^{\frac{q(v_2+I_2R_s)}{n_1 kT}} - 1\right) - I_{02}\left(e^{\frac{q(v_2+I_2R_s)}{n_2 kT}} - 1\right) - \left(\frac{v_2+I_2R_s}{R_{sh}}\right) - a\left(v_2+I_2R_s\right)\left(1-\frac{v_2+I_2R_s}{V_{br}}\right)^{-m} \quad (8)$$

$I_{ph,1}$ and $I_{ph,2}$ are the photo-current of normal cells and shaded cells. the shading percentage B of the cell, is given according to Eq.(9).

$$I_{ph,2} = \beta . I_{ph,1} \tag{9}$$

In Eq. (8) a is a correction factor and m an exponent of avalanche breakdown.

3. Detection and localization Method

A monitoring system must achieve three main tasks, detection which consist to take a binary decision, either the system works properly or a failure occurred.

The localization, its role is to determine the defective components; the identification consists of determining the shape of the failure in order to determine the nature of maintenance or correction that should be made.

Recent approaches offer new types of PV panels connections other than the standard serial and parallel connections and by adding a certain number of current and voltage sensors. The comparison of these currents, leads to locate the location of the photovoltaic panels that are faulty. The use of certain fusion rules of data help

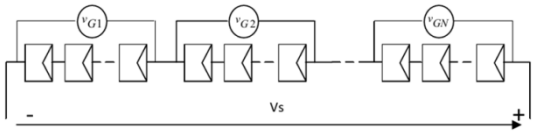

Fig.4. Structure of a PV string and the connected voltage sensors on each group

To improve the decision making and the fault localization, these methods are not effective on conventional connections [18, 19].

In order to overcome this problem, the proposed method of faults detection and localization is to use a minimum number of voltage sensors in a group of panels, connected in a classical way presented as a string of N series groups, figure 4.

The total voltage delivered by the string is given by the following equation:

$$V_s = \sum_{i=1}^{N} v_{Gi} \tag{10}$$

V_S is the voltage with a string, v_{Gi} is the voltage delivered by a group. In the case of normal operation (D = 0), the tension of a group is given by the following equation:

$$v_{Gi} = n.v \tag{11}$$

With v is the voltage panel, n is the number panel in a group, In the case of a defect (D = 1) in a group, the voltage of the group will be as follows:

$$v_{Gi} = (n-k).v + \sum_{j=1}^{k} v_k \tag{12}$$

Or k is the number of panels in a failure in a group, v_k is the voltage of the defected panel, D is the signal of the absence or presence of the defect and j is the number of defected panels.

To fulfill the detection and localization, we have to compare the measured voltages v_{Gi} of each group with a threshold S calculated from the model equations depending on weather conditions and on the uncertainties of the system and instrumentation measures.

$$S = v_{Ge} - \varepsilon \tag{13}$$

v_{Ge} is the estimated tension of the group, ε is the uncertainty on the system and the measures instrumentation.

The decreases of v_{Gi} voltage below the threshold makes the fault signal D equivalent to 1, which means that the group i is defected.

4. Failure identification by analyzing the I-V characteristic

In this section, we will exploit the variation of the I-V characteristic to identify a partial shade defect and a significant change in series resistance. This change can be expected when there is a change of state of PV array caused by changes in operating conditions (temperature and irradiation) or an appearance of defects in the PV array.

Among the symptoms of a failure, generated by partial shading and series resistance is the presence of one or several inflection points in the I-V curve. These inflection points result from the conduction of one or more bypass diodes. This conduction causes a sudden loss of the voltage of the cell group for a very small variation of the current.

By using the I-V characteristics of the defected PV array, the identification of defects can be achieved. Such an analysis is already in some studies in the literature, when the derivative of the voltage relative to the current allows the identification of the defect [20-22].

If ΔV is the difference between the characteristic with and without defect. The calculation of $\max\left(\frac{d^2\Delta V}{dI^2}\right)$ will allow us to verify the presence of inflection points. Several results showed that in the case of partial shade defect, the $\max\left(\frac{d^2\Delta V}{dI^2}\right) > 0$ and in the case of a significant change in series resistance, the

$\max\left(\frac{d^2\Delta V}{dI^2}\right) = 0$ [22].

The following figures show the shape of I-V characteristic of a failed PV panel operation (shading, series resistance) compared with normal operation.

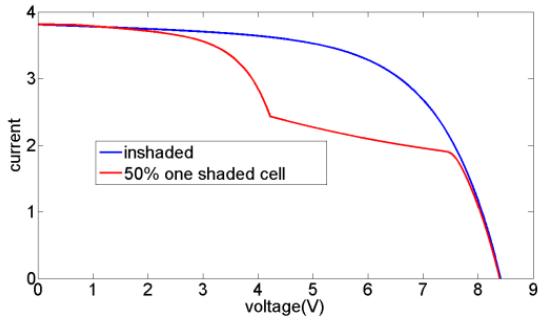

Fig.5. IV characteristics with and without defect

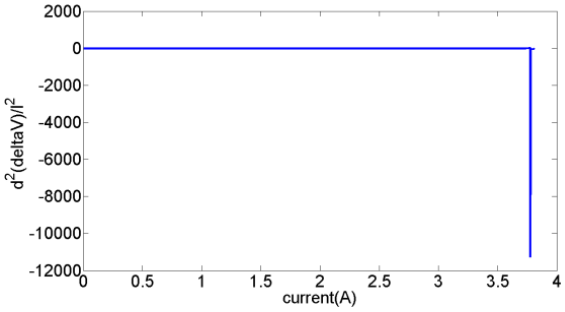

Fig.6. second derivative of the voltage error without defect

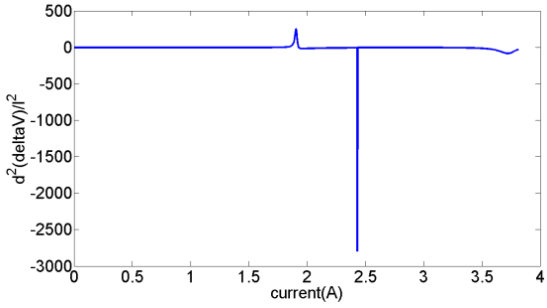

Fig.7. second derivative of the voltage error with defect with and without defect

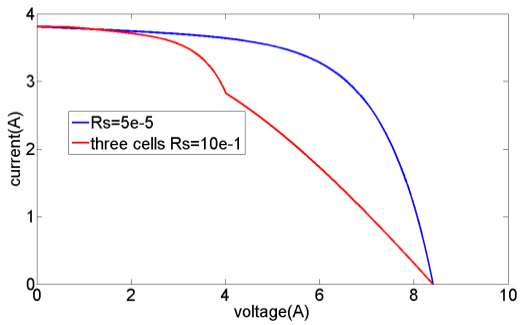

Fig.8. IV characteristics with and without defect

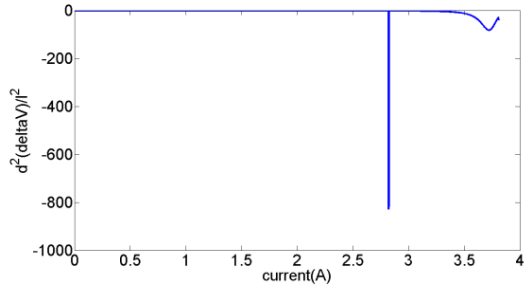

Fig.9. second derivative of the voltage error with defect

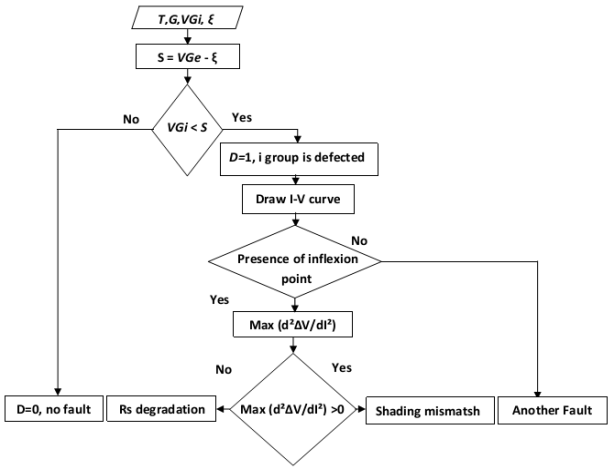

Fig.10. fault diagnosis flowchart for partial shading and significant increasing in the series resistance

5. Results and discussion

To validate the proposed diagnosis procedure, we consider a string consists of fifteen PV panels connected in series. This string is composed in turn of three groups.

Each group consists of five panels. For the simulation, we have considered the following defects:

- A partial shading defect of 75% on a cell in group G_2.
- A partial shading defect of 100% on a cell in group G_1 and another of 50% for group G_2.
- A series resistance defect in group G_3 (variation of Rs= 5e-5 to 10e-1 for five – cells in a group).

Simulation results are obtained using the Matlab software and under the following weather conditions: Solar irradiation G = 1 kW/m2 and temperature Ta ° = 298.15k.

5.1. Partial shading of 75% on a one cell in group G_2

In order to simulate the effect of partial shading on the I-V characteristic, the previously presented dual diode model is used. Fig. 11 shows the characteristic in the case without fault and in the case of a partial shade in a group.

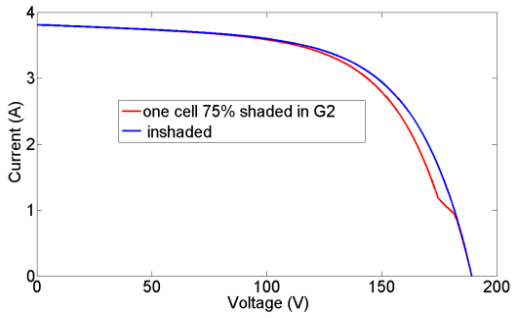

Fig.11. characteristics with and without defect

For detection and localization steps, we have to compare the VGI voltage from each group with a threshold S.

From Fig. 13, it is clear that the group G_2 is in defect because the voltage VG_2 is below the threshold voltage. The other groups have no defects.

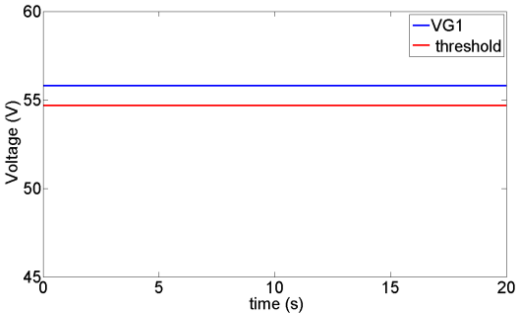

Fig.12. Voltage of group G_1 and the threshold for fault detection

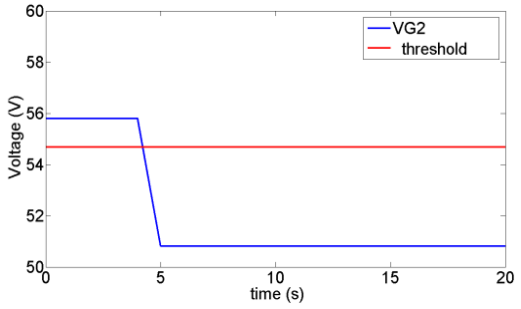

Fig.13. voltage of group G_2 and the threshold for fault detection

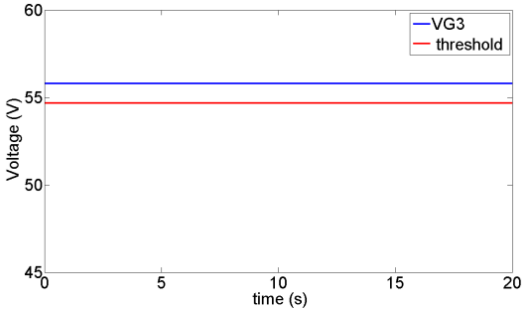

Fig.14. voltage of group G_3 and the threshold for fault detection

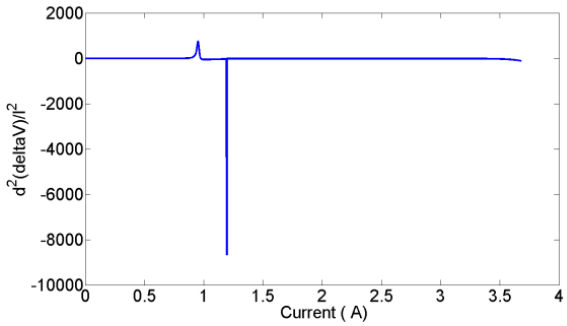

Fig.15. second derivative of the voltage error with defect

It is clear from fig. 11 and fig. 15 that the I-V characteristic has an inflection point which is the consequence of a defect of partial shading or a variation on the series resistance. The application of the diagnosis procedure of the flowchart of fig. 10 shows that $\max\left(\frac{d^2\Delta V}{dI^2}\right) = 644.9623$ therefore $\max\left(\frac{d^2\Delta V}{dI^2}\right) > 0$ which confirms the presence of a partial shading defect.

5.2. Partial shading of 100% on a cell in group G_1 and another of 50% in group G_2.

In this section, we will consider the presence of two faults; the first is a complete shading of a cell in a panel in group G_1 and another of 50% in group G_2. Fig. 16 shows the shape of the characteristic with and without defect. The characteristic defect contains two clear inflection points.

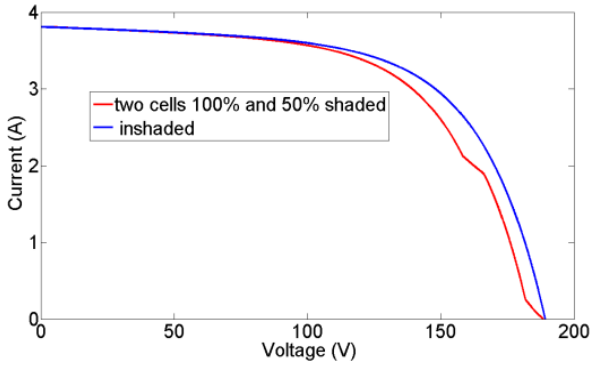

Fig.16. The I-V characteristics with and without default.

In the same way as the previous section, the application of the diagnosis algorithm confirmed that the group G_1 and group G_2 are in defect and the threshold voltage S = 41.71v.

The voltage of Group G_1 and Group G_2 after the fault appearance are: VG_1 = 47.0934 and VG_2 = 50.8750.

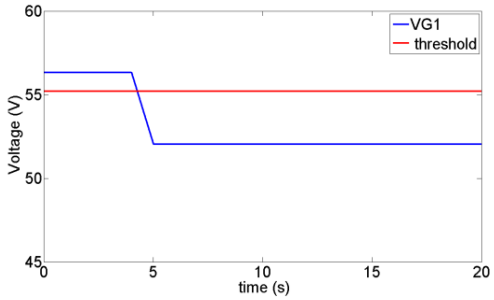

Fig.17. voltage of group G_1 and the threshold for fault detection.

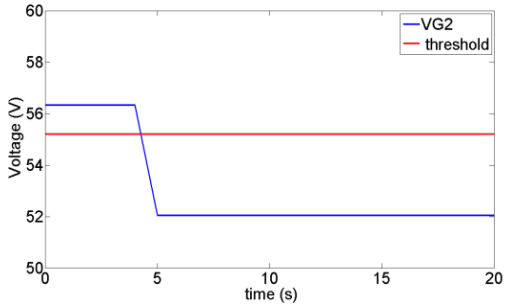

Fig.18. voltage of group G_2 and the threshold for fault detection.

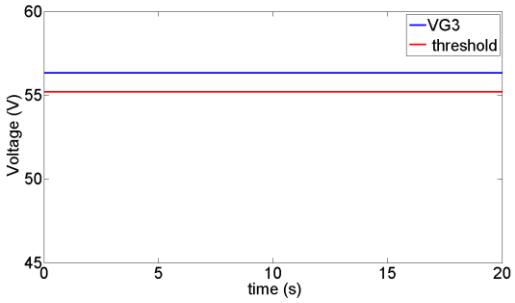

Fig.19. voltage of group G_3 and the threshold for fault detection.

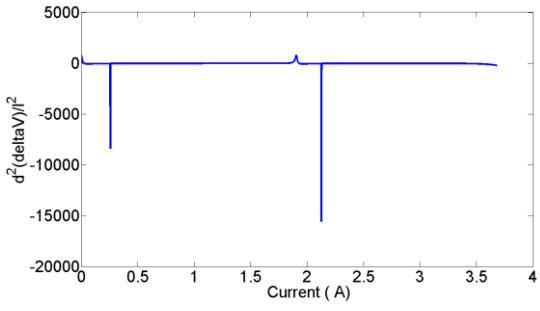

Fig.20 second derivative of the voltage error with default.

From Fig. 20, we have two inflection points, the $\max\left(\frac{d^2\Delta V}{dI^2}\right) = 643.6879$ which means the partial shading defect.

5.3. Defect of series resistance in G_3

Among the defects which cause an inflection point in the characteristic I-V, is the change in series resistance in a photovoltaic panel. The following figure shows the characteristic of a string made up of three groups. A defect of series resistance type in the group G_3 is considered.

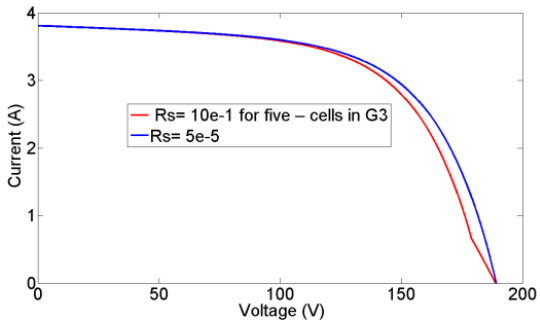

Fig.21. IV characteristics with and without defect.

the Figs. 22, 23 and 24 shows the shape of detection and location signals, the change in the voltage VG_3 caused by the defect of the series resistance makes a reduction of this voltage below the threshold , therefore the detection and localization of this defect.

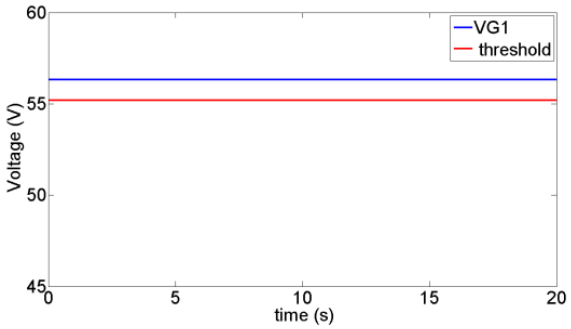

Fig.22. voltage of group G_1 and the threshold for fault detection.

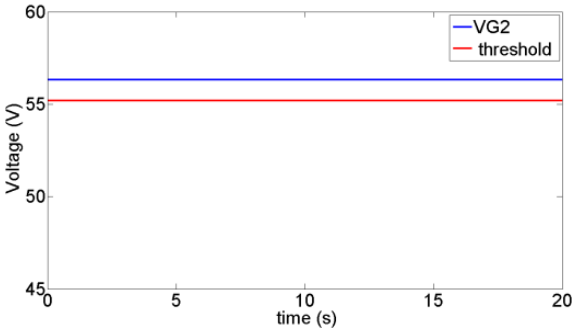

Fig.23. voltage of group G_2 and the threshold for fault detection.

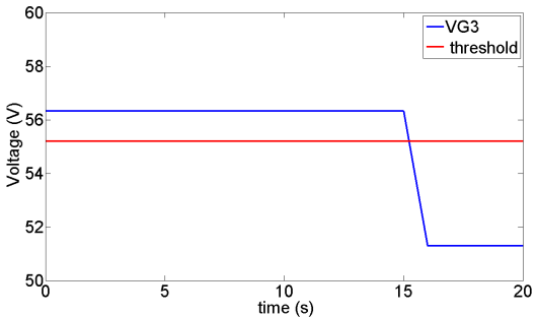

Fig.24. voltage of group G_3 and the threshold for fault detection.

From Fig. 25, $\max\left(\frac{d^2\Delta V}{dI^2}\right)=0$, Thus, the detected fault is a fault-type series resistor.

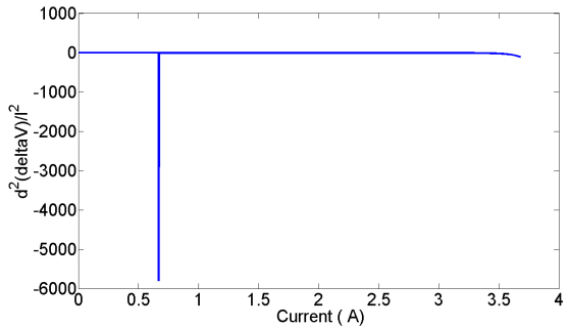

Fig.25. Second derivative of the voltage error with default.

6. Conclusions

In this paper, a new automatic method of detecting and locating physical and electrical degradation in the photovoltaic cell combines the use of minimum voltage sensors and analysis of the I-V curve. The application of this method to groups composed of five panels and comparing the voltages of each group to a threshold voltage allows detecting and locating the fault. The identification of the faults is performed by the analysis of the presence of inflexions points in the IV curve.

The obtained simulation results showed The Effectiveness of the proposed method and the model used. In perspective, the implementation of our algorithm in an experimental test bench is considered.

References

[1] A. Eddiai, M. Meddad, D. Guyomar, A. Hajjaji, Y. Boughaleb, K. Yuse, S. Touhtouh, B. Sahraoui. Synthetic Metals, **162**, 1948 (2012).

[2] A. Eddiai, M. Meddad, S. Touhtouh, A. Hajjaji, Y. Boughaleb, D. Guyomar, S. Belkhiat, B. Sahraoui. J. Appl. Phys. **111**, 124115 (2012).

[3] M. Meddad, A. Eddiai, A. Hajjaji, D. Guyomar, S. Belkhiat, Y. Boughaleb, A. Chérif. Optical Materials, **36**, 80 (2014).

[4] E. Kaplani. International Journal of Photoenergy, D (2012). doi:10.1155/2012/396792.

[5] R. Kadri, H. Andrei, J.P. Gaubert, T. Ivanovici, G. Champenois, P. Andrei. 8th World Energy System Conference. WESC 2010.Energy **42**, 57 (2012).

[6] R. Chowdhury, H. Saha. Solar Energy Materials & Solar Cells, **94**, 1441 (2010).

[7] K.H. Chaoa, S.H. Hob, M.H. Wang. Modeling and fault diagnosis of a photovoltaic system **78**, 97 (2008).

[8] A.S Chouder, Silvestre, N. Sadaoui, L. Rahmani. Simulation Modeling Practice and Theory, **20**, 46 (2012).

[9] E. Karatepe, M. Boztepe, M. Colak. Solar Energy **81**, 977 (2007).

[10] J.I. Rosell M. Ibanez. Energy Conversion and Management **47**, 2424 (2006).

[11] S. Yadir, M. Benhmida, M. Sidki, E. Assaid, M. Khaidar. International Conference on Microelectronics (ICM) (2009).

[12] C. Carrero, J. Amador, S. Arnaltes. Renewable Energy, **32**, 2579 (2007).

[13] K. Ishaque, Z. Salama, Taheri, H. Syafaruddin. Simulation Modelling Practice and Theory **81**, 1613 (2011).

[14] P. Singh, S. Singh, N. Lal, M. Husain. Solar Energy Materials and Solar Cells **92**, 1611 (2008)

[15] A. Zegaouia, P. Petita, M. Ailleriea, J.P Sawickia, A.W. Belarbi, M.D. Krachai, J.P. Charles. Energy Procedia **6**, 695 (2011).

[16] H. Kawamura, K. Naka, N. Yonekura, S. Yamanaka, H. Kawamura, H. Ohno, K. Naito. Solar Energy Materials and Solar Cells, **75**, 613 (2003).

[17] G. Notton1, I. Caluianu, I. Colda, S. Caluianu. Revue des Energies Renouvelables **13** ,49 (2010).

[18] Y. Liu, B. Li, Z. Cheng. In: International Conference on Control and Decision Conference. CCDC2010. Tianjin. China, (2010).

[19] Z. Cheng, D. Zhong, Y. Li, B. Liu. In: International Conference on Power and Energy Engineering Conference. APPEEC 2011. Tianjin. China (2011).

[20] M. Miwa, S. Yamanaka, H. Kawamura H. Ohno. Conference Record of the IEEE 4th World Conference, Meijo Univ. Nagoya (2006).

[21] T. Mishina, H. Kawamura, S. Yamanaka, H. Ohno, K. Naito. Photovoltaic Specialists Conference IEEE. Nagoya. Japan (2002).

[22] L. Bun. Ph.D, thesis, Dept. Génie Electrique, Université De Grenoble France (2011).

* Corresponding author: aeddiai@gmail.com